Industrial Engineering Journal
ISSN: 0970-2555
Volume : 54, Issue 10, October : 2025

AN ADAPTIVE DUAL INPUT-DUAL OUTPUT CONVERTER WITH NON-ISOLATED FEATURES FOR USE IN ELECTRIC VEHICLE

[1] Lavudi Sindhu Rani [2] Dr. D. Kiran Kumar
Department of Electrical and Electronics Engineering, JNTUHUCEST, Hyderabad, India
Email: [1] :sindhu.sindhurani345@gmail.com, [2]kirannkumar9@jntuh.ac.in

Abstract— A variety of power electronics applications have recently made use of dc/dc converters with high voltage conversion. Electric car and DC microgrid solutions are centred on multi-port converter topologies. This article primarily focusses on the new non-isolated four-port (two input and two output) power electronic interface structure that can be utilised in electric vehicle (EV) applications. Mainly, this converter can deal with power sources that have different characteristics in terms of voltage and current.

During its operation, the suggested architecture is capable of producing both buck and boost outputs simultaneously. Increased reliability and efficiency are achieved by implementing the proposed four-port converter (FPC) with fewer components and a more straightforward control method. The converter's bidirectional power flow capability also makes it a good fit for regenerative braking electric vehicle battery recharge. We analyse the converter's steady-state and dynamic behaviour and present a control approach to govern the power flow between the several energy sources. An extracted small-signal model is used to create the converter that is suggested. The modelling and testing results in MATLAB, along with the results from various operating modes, validate the converter design and establish its performance behaviour.

Keywords: Bidirectional dc/dc converter, electric car, multi-port converter, battery storage, and regenerative charging Modeling with MATLAB/Simulink.

I.INTRODUCTION

These days' cars are to blame for a lot of problems, like rising petrol prices, more pollution, higher temperatures, and the eventual exhaustion of fossil fuels. Environmentally friendly electric and hybrid vehicles (HEVs) have so been produced by the automotive industry. This vehicle's motor drive system is a crucial part. An effective power electronic converter powers the motor drive system. For electric vehicles to function, this power electronic converter has to communicate with the vehicle's battery and motor control systems. Electric vehicle systems' power electronic interfaces have been the subject of substantial study and published reports. A number of non-isolated three-port converter topologies are covered, including DIC/DOC and SISO converter topologies.

A step-up converter that combines buck-boost and KY converters is known as a voltage conversion ratio-rich converter. Isolated bidirectional converters are known as multiport dc/dc converters.

The converter is enlarged by a multi-winding transformer, which serves to simplify the transfer of electricity. By integrating dc-link, many multiport bidirectional dc/dc converter topologies can be achieved. together with magnetic coupling. The operation of a SISO converter is identical to that of a full-direction universal dc-dc converter. The hybrid electric vehicle is designed to work with converters that

Industrial Engineering Journal
ISSN: 0970-2555
Volume : 54, Issue 10, October : 2025

have two inputs and two outputs. The lack of an improvement in battery power caused by the load is the primary drawback.

A fuzzy logic control–based energy management approach has been suggested to improve power management between the battery and the ultracapacitor, thereby avoiding problems like high battery current during peak power and overcharging the ultracapacitor. A four-port (FPC) three-switch, single-stage, transformer-less, bidirectional buck boost converter is the primary output of this research. The suggested converter may combine many sources with varying input voltage and current characteristics, and its modular construction makes it easier to manufacture with fewer parts.

Along with the previously mentioned characteristics, the converter that has been presented can also provide an output that is either higher than or lower than the maximum input voltage (boost) or lower than the minimum input voltage (buck).

The efficiency of the suggested converter is enhanced by the decrease in switching losses.

Below is the document's organisational structure. Part I: Introduction. Part II: The Fundamental Concept Behind FPC Development. The third section covers the operational modes. Section Section IV: Controller and Integration Implementation

The Suggested Four-Port Converter's Control Strategy In Section V, we see some examples of how the features of the proposed converter were tested using experimental data and a power budgeting control technique. Final thoughts in Section VII. Works Cited.

II.Analysis of Multiport Buck-Boost Convertor Performance

2.1 The FPC topological framework

An electric vehicle system's fluctuating input power and dynamic load make it impossible to meet load requirements with a single energy source. Therefore, it is necessary to hybridise all energy resources.

The main goal is to create a converter architecture that can link different energy sources to the powertrain of a vehicle.

The function of the power electronic interface in an electric vehicle's power system is shown in Figure 1.1(a) and (b).

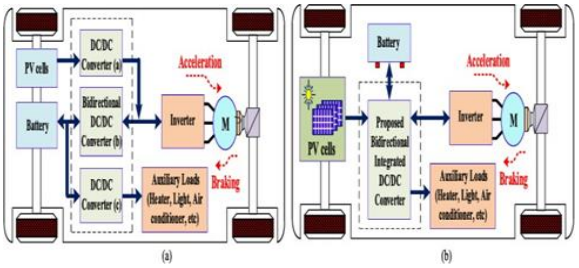

Figure 2.1 shows the proposed FPC interface for electric car systems in block diagram form, which combines classic converter (a) with integrated four-port (b).

The notable features of the recommended converter are:

- The capability of bidirectional electrical transfer.
- Oversight of the independent power flow between generators A straightforward process for design, control, and execution
- If you have a DC input voltage and want to convert it to DC voltage, you need a DC-to-DC converter. The levels of the input and output voltages are typically different. Among the many other uses for DC-to-DC converters are noise isolation and power bus regulation. Several common DC-to-DC converter topologies are detailed in this article.

Industrial Engineering Journal
ISSN: 0970-2555
Volume : 54, Issue 10, October : 2025

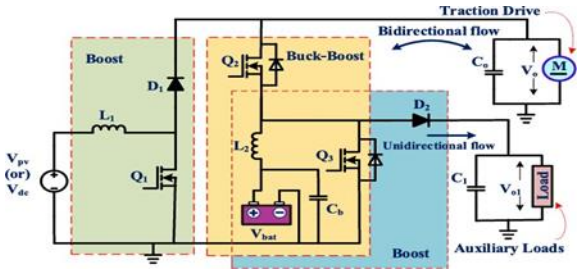

Figure 2.2 shows the suggested setup for a four-port converter (FPC).

2.2 BUCK CONVERTER

With the transistor activated, voltage Vin is applied to one end of the inductor in this circuit.

Although the transistor is turned off, the current will still flow through the inductor and now go through the diode since the inductor current tends to climb with this voltage.

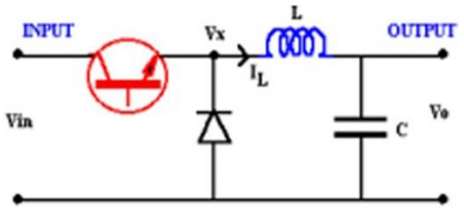

Fig.2.3 Buck Converter

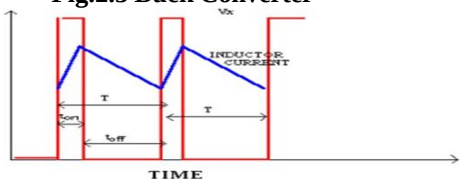

Fig:2.4. Voltage and current changes

Examining the inductor current's evolution through a single cycle will provide light on the circuit's voltages. When thinking about the connection

$$di$$

$$Vx - V0 = L\,dt$$

$$di = \int (Vx - V0)\,dt + \int \quad (Vx - V0)$$

ON OFF

There is a satisfactory change in current

2.3 BOOST CONVERTER

A simplified diagram of the boost converter is shown in Figure 2.5. When the output voltage needs to be higher than the input voltage, this circuit is utilised.

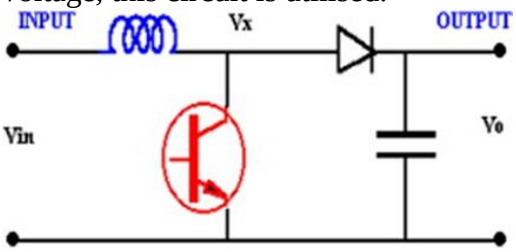

Fig.2.5: Boost Converter Circuit

III. OPERATION STATE AND MODES OF OPERATION SIDO (SINGLE INPUT DUAL OUTPUT)

In this configuration, PV delivers power to the load independently. Between the timestamps 0 and d1Ts, the switches Q2 is in the off state while Q1 and Q3 are in the on state. Figure 5(a) and (b) show that the inductor current increases with a positive slope when Vpv>Vbat, since the

voltage Vpv occurs across the inductor L1.During the time span d1Ts to Ts, switches Q2 are turned on while switches Q1 and Q3 are toggled off. The energy accumulated in inductor L1 during the previous time interval d1Ts is transferred to the current through diode D1.

$$V_0 = \frac{1}{1 - d_1} V_{pv} \qquad (1)$$

$$V_{01} = \frac{1}{1 - d_1} V_{pv} \qquad (2)$$

2) SITO (SINGLE INPUT THREE OUTPUT)

STATE 2.

POWER TRANSFER FROM PV TO BATTERY AND LOAD STATUS OF THE CONVERTER

Q2 works with d2 < 05 to charge the battery when it has to be charged from PV (see Figure 5(c) and (d)). With d1 > 05, Q3 functions similarly to Q1 to generate

Industrial Engineering Journal
ISSN: 0970-2555
Volume : 54, Issue 10, October : 2025

increased output across the load. The relationship between the voltages Vbat, Vpv, and Vo, Vo1 is

$$V_0 = \frac{1}{1-d_1} V_{pv} \quad (3)$$

$$V_{01} = d_2 V_{pv} \quad (4)$$

$$V_{bat} = d_2 V_{pv} \quad (5)$$

3) CONVERTER STATE 3-SIDO STATE (POWER TRANSFER FROM THE BATTERY)

In this condition, the load receives the energy that the battery has stored. The inductor current iL2 increases linearly as a result of the battery's discharging action between 0 and d3Ts. The present iL2 declines with a negative slope between the intervals d3Ts to Ts. The switch's ON/OFF status The drive train's overall output is increased by Q3. Q1 is maintained in OFF mode during operation since it does not participate in the process of transferring energy from the battery to the load (see Figure 5(e) and (f)). When the battery is discharged, the output voltage across the load is provided as

$$V_0 = \frac{1}{1-d_3} V_{bat} \quad (6)$$

$$V_{01} = \frac{1}{1-d_3} V_{bat} \quad (7)$$

4) THE CONVERTER'S STATE 4 DIDO (DUAL INPUT DUAL OUTPUT) STATE (POWER TRANSFER FROM PV AND BATTERY)

Figure 5(g) and (h) show that when the electric vehicle's power consumption is large, the power is supplied by the battery and PV. In order to charge the inductor, the currents iL1 and iL2 rise linearly between 0 and d1Ts, caused by gated switches Q1 and Q3. Here, Q2 receives the corresponding gate signal. In contrast, when switches Q1 and Q3 are not in use, the inductor currents iL1 and iL2 fall in a negative slope.

$$V_0 = \frac{1}{1-d_1} V_{pv} \quad (or) \qquad V_0 = \frac{1}{1-d_3} V_{bat} \quad (8)$$

$$V_{01} = \frac{1}{1-d_1} V_{pv} \qquad (or) \quad V_{01} = \frac{1}{1-d_3} \quad (9)$$

STATE 5-POWER TRANSFER FROM LOAD TO BATTERY: SIDO STATE OF THE CONVERTER

The drive train's stored kinetic energy is transferred back to the battery during regenerative braking (see Figure5(i) and (j)). The following is the state's switching sequence: While Q2 and Q3 are turned ON and OFF, respectively, Q1 remains permanently in the off state. The battery is charged by Q2 and Q3 in their ON-OFF states.

$Vbat = d2V0$ (10)

In the same condition, the second output uses regenerative braking power to replace the battery. The control relationship can be obtained as

$V_{01} = d_3 V_0$ (11)

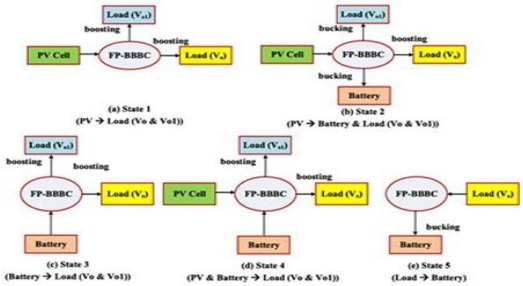

Fig.3.1: a) State 1(boost), b) State 2 (buck & boost), c) State 3 (boost), d) State 4 (boost), e) State 5 (buck).

Industrial Engineering Journal
ISSN: 0970-2555
Volume : 54, Issue 10, October : 2025

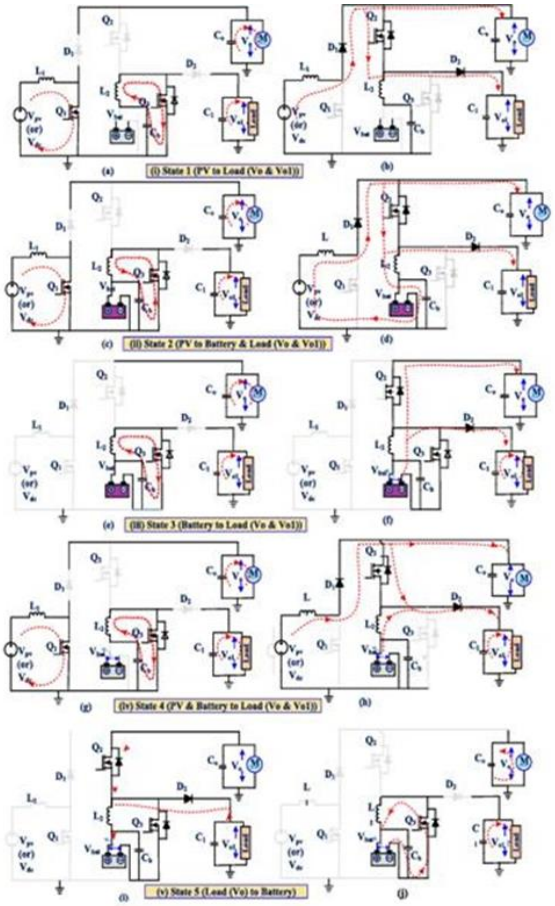

Fig.3.2: Typical diagram of all the states (i)State1, (ii)State2, (iii)State3, (iv)State4, &(v)State5

Operational conditions

No.of States	Input Sources	MOSFET Switches			Inductors		Diodes		Battery	Capacitors		Outputs	
		Q_1	Q_2	Q_3	L_1	L_2	D_1	D_2	$V_{bat}(or)\,C_b$	C_o	C_1	(V_o)	(V_{ol})
State 1 ($V_{pv}>V_{bat}$)	(V_{pv}) or (V_{ab})	ON	OFF	ON	↑	↑	OFF	OFF	·	↓	↓	Boost	Boost
		OFF	ON	OFF	↓	↓	ON	ON		↑	↑		
State 2 ($V_{pv}>V_{bat}$)	(V_{pv}) or (V_{ab})	ON	OFF	ON	↑	↓	OFF	OFF	↑	↓	↓	Boost	Boost
		OFF	ON	OFF	↓	↑	ON	ON		↑	↑		
State 3 ($V_{pv}<V_{bat}$)	(V_{bat})	·	OFF	ON	·	↑	·	OFF	↓	↓	↓	Boost	Boost
		·	ON	OFF	·	↓	·	ON		↑	↑		
State 4 ($V_{pv}=V_{bat}$)	(V_{pv}) and (V_{bat})	ON	OFF	ON	↑	↑	OFF	OFF	↓	↓	↓	Boost	Boost
		OFF	ON	OFF	↓	↓	ON	ON		↑	↑		
State 5 ($V_{pv}=0$, $V_{bat}<V_{bat}$)	Regenerative braking power	·	ON	OFF	·	↑	·	ON	↑	↓	↓	Buck	Buck
		·	OFF	ON	·	↓	·	OFF		↑	↑		

Table representation: ON- Switch close. OFF- Switch open, ↑- charging of inductor and capacitor, and ↓- discharge of inductor and capacitor

Table. 1

IV. CONTROL STRATEGY

4.1 PI CONTROLLER

A proportional integral derivative (PID) control can also be implemented using just the proportional and integral terms. When it comes to controller types, the PI controller is even more popular than full PID controllers. The value of the controller's output, u(t), is the altered variable input that the system receives**.**

e(t)=SP-PV

u(t)=ubias+Kce(t)+Kc$\tau I \int t0e(t)dt$

4.2 DISCRETE PI CONTROLLER

Since digital controllers use discrete sample periods, the integral of the error must be estimated using a discrete variant of the PI equation. Here, nth represents the number of samples and Δt is the interval between each sample. The integral's continuous form is replaced by a sum of the mistake. u(t)=ubias+Kce(t)+KcτInt∑i=1ei(t)Δt

ADVANTAGES AND DISADVANTAGES

A PI controller's steady-state error is zero because of the integral term, which is not the case with proportional-only control in general. Without derivative action, the system may be more stable in steady state when dealing with noisy data. For one thing, derivative behaviour is more affected by input variables with higher frequencies.

4.3 INTEGRAL ACTION AND PI CONTROL.

A controller output (CO) signal is calculated and sent to the ultimate control device (such a valve or variable speed) by the Proportional-Integral (PI) algorithm.pump), just as the P-Only controller does at each sample time T. In the PI method, the controller error, denoted as e(t), and the parameters used for tuning the controller have an impact on the

Industrial Engineering Journal
ISSN: 0970-2555
Volume : 54, Issue 10, October : 2025

calculated output.

4.4 FUZZY LOGIC CONTROLLER

FLC takes in two signals and outputs one. The three components are the control signal, the error change (de), and the error (e). Linguistic variables, which represent inputs and outputs, can be grouped into the following kinds: NB, NM, NS, Z, PS, PM, and PB. The normalisation range for all inputs and outputs is 10, as can be observed. The fuzzy sets were described using the following terms: "Negative Big" (NB), "Negative Medium" (NM), "Negative Small" (NS), "Zero" (Z), "Positive Small" (PS), "Positive Medium" (PM), and "Positive Big" (PB). Decision rules can be assigned according to the ones shown in Table IV.

Human intuition and prior knowledge of the process form the basis of the fuzzy rules. These rules comprise the input/output links that define the control strategy. Since there are seven fuzzy sets in each control input, the maximum number of fuzzy rules is 49.

CE E	NB	NM	NS	Z	PS	PM	PB
NB	NB	NB	NB	NB	NM	NS	Z
NM	NB	NB	NB	NM	NS	Z	PS
NS	NB	NB	NM	NS	Z	PS	PM
Z	NB	NM	NS	Z	PS	PM	PB
PS	NM	NS	Z	PS	PM	PB	PB
PM	NS	Z	PS	PM	PB	PB	PB
PB	Z	PS	PM	PB	PB	PB	PB

Table 2: Table of FUZZY Rules

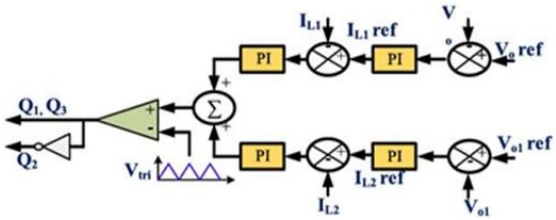

Fig:4.1 Proposed FPC PWM generator with PI control

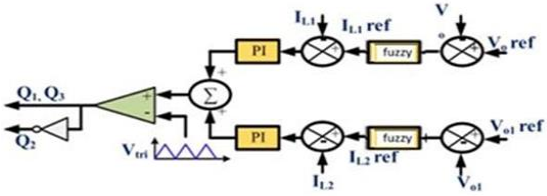

Fig.4.2 Proposed FPC PWM generator with Fuzzy logic control

V. SIMULATION CIRCUITS AND RESULTS

Complete model implementation and MATLAB/Simulink simulation were conducted to assess the efficacy of the suggested Dual Input Dual Output Four Port Converter.

The construction of the four-port converter requires only three MOSFET switches, namely Q1, Q2, and Q3. A direct current (DC) power source or a battery can power the input. From the converter, you can choose between a main and an auxiliary output, depending on your needs.

The converter can also buck and raise the voltage at the output. During regenerative braking, the drive train's stored kinetic energy is transferred back to the battery, enabling regenerative operation.

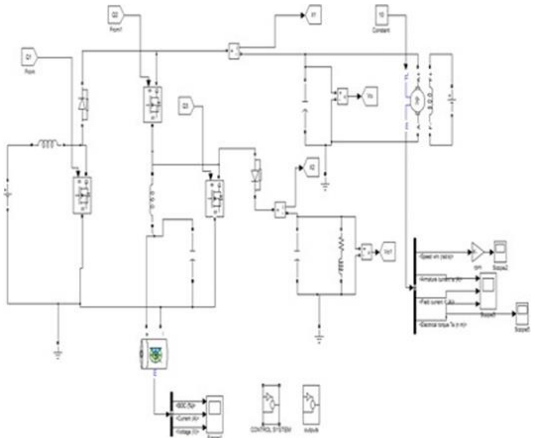

Fig: 5.1. Simulink Model of a Multifunctional Non- Isolated Dual Input-

Industrial Engineering Journal
ISSN: 0970-2555
Volume : 54, Issue 10, October : 2025

Dual Output Converter

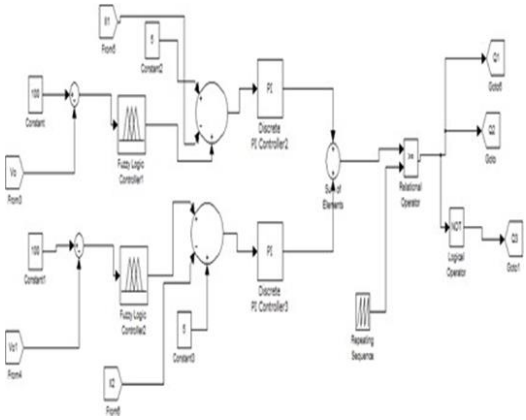

Fig:5.2. Simulink Model of a Control Circuit

To keep errors to a minimum, the control circuit compares the current voltage to a 100V reference using a fuzzy logic controller. With PI Controller, the research state error can be minimised. In order to acquire a digital signal, one must first acquire a sawtooth or triangle signal with carrier reference.

Parameters	Volts
Dc Voltage source	100V
Inductor (L1)	1mH
Inductor (L2)	120µH
Capacitor (C1)	1µF
Capacitor (C2)	1000µF
Load Resistance	1Ω
Load inductance	1mH

Table 3: Model Specifications.

Parameters	Value
Nominal Voltage	12V
Number of batteries	1
SOC	99.5%
Rated capacity	7Amp/hr

Table 3: Battery Specifications

5.1 SIMULATION RESULTS

SIMULATION RESULTS WITH FUZZY LOGIC CONTROLLER

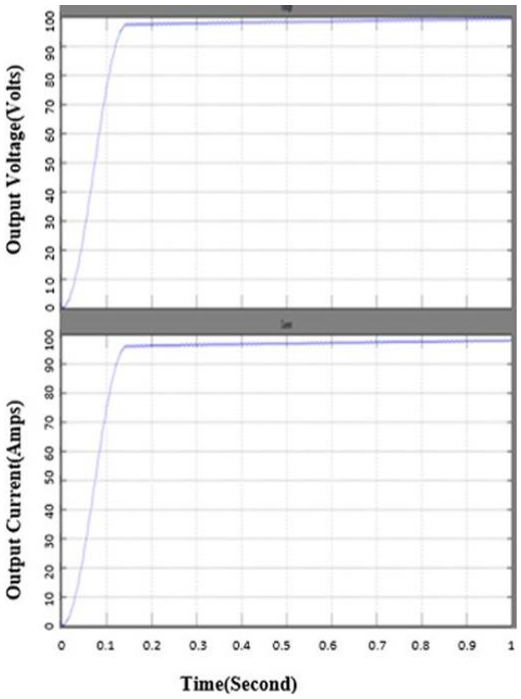

Output waveforms of a voltage and current across Main load with Fuzzy Logic Controller.

Industrial Engineering Journal
ISSN: 0970-2555
Volume : 54, Issue 10, October : 2025

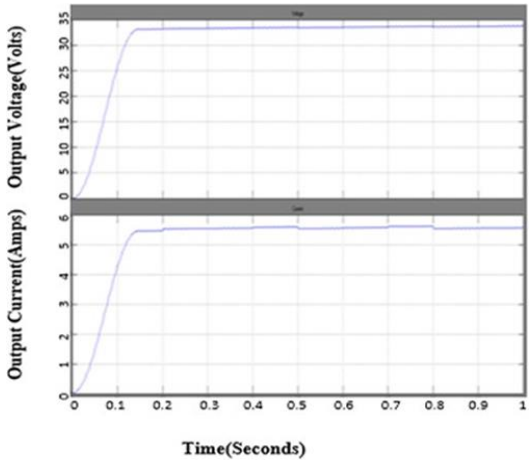

Output waveforms of a voltage and current across Auxiliary Load with Fuzzy Logic Controller.

The input voltage of 21 volts is brought down to 35 volts by means of a buck operation after being increased to 100 volts. The fuzzy logic creates an output voltage that is ripple-free computer programmer.

SIMULATION RESULTS WITH PI CONTROLLER

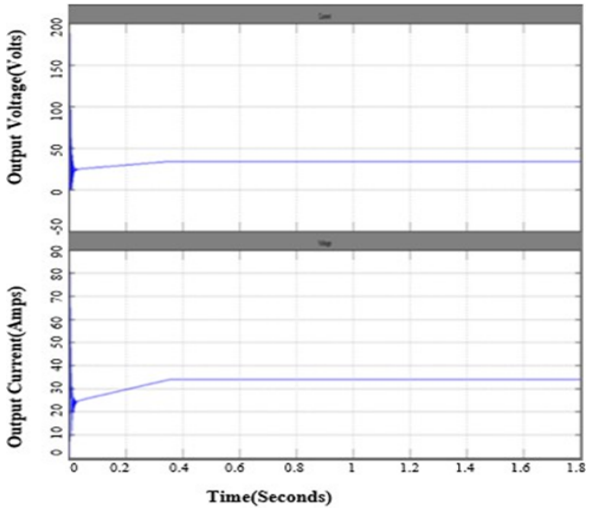

Output waveforms of a voltage and current across Main load with PI Controller.

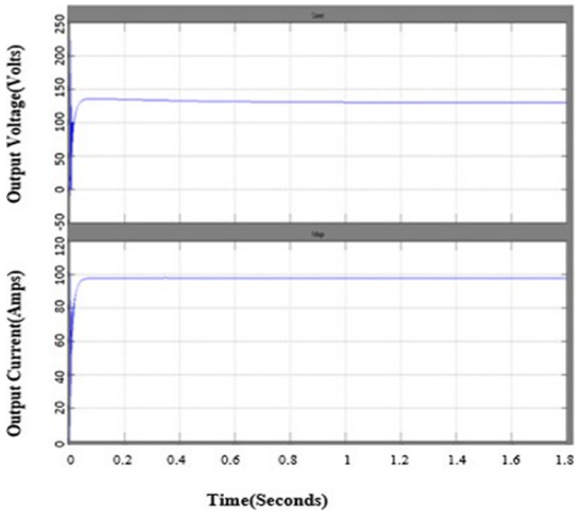

Output waveforms of a voltage and current across Auxiliary load with PI Controller.

The output voltage is boosted and buck-boosted by the PI Controller during first transients. This early transient can be mitigated by incorporating a fuzzy logic controller into the control circuit design.

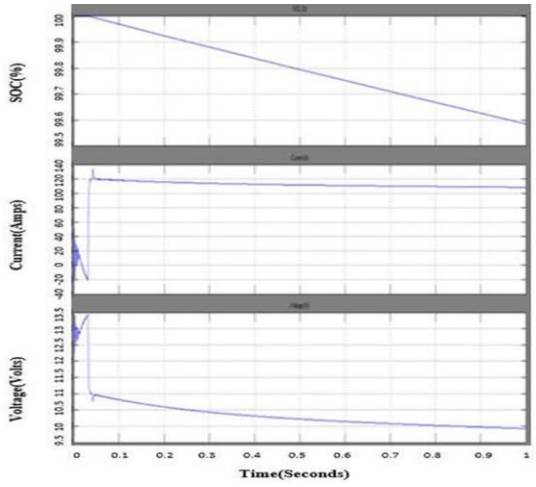

State of charge (SOC), Voltage & Current of the battery

The battery will enter a 99.5 state of charge when it stops conducting, which happens when the continuous DC source is conduction. Over the battery, the current is 110A and the voltage is 10V**.**

5.2 A comparison between the suggested fuzzy controller and the conventional pi controller.

Topology	Rise time	Settling time
Conventional pi controller	0.005sec	0.31sce
Proposed fuzzy controller	0.056sec	0.14sec

V.CONCLUSION

One possible component of an electric vehicle hybridisation technique is a single-stage four-port (FPC) buck-boost converter, according to this research. This converter has several advantages over other buck-boost converter topologies that have been discussed in the literature: A) it can manage many resources with varying voltage and current capabilities; b) it can provide buck, boost, or buck-boost output without an additional transformer; and c) it can have bidirectional power flow capabilities with fewer elements.

Analytical mathematics has shown the suggested converter's functionality. A simple control approach has been settled upon for the purpose of allocating input power budgets. Now we can use the Simulink model to confirm that the converter works as expected. Using simulation findings, we can confirm that the four-port buck-boost architecture is feasible.

REFERENCES

1. H. Wu, Y. Xing, Y. Xia, and K. Sun, ‘‘A family of non isolated three-port converters for standalone renewable power system,’’ IEEE Trans. Power Electron., vol. 1, no. 11, pp. 1030–1035, 2011.
2. K. I. Hwu, K. W. Huang, and W. C. Tu, ‘‘Step- up converter combining KY and buck-boost converters,’’ Electron. Lett., vol. 47, no. 12, pp. 722–724, Jun. 2011.
3. H. Xiao and S. Xie, ‘‘Interleaving double-switch buck boost converter,’’ IET Power Electron., vol. 5, no. 6, pp. 899–908, Jul. 2012.
4. H. Kang and H. Cha, ‘‘A new nonisolated High-Voltage Gain boost converter with inherent output voltage balancing,’’ IEEE Trans. Ind. Electron., vol. 65, no. 3, pp. 2189–2198, Mar. 2018.
5. T. Bang and J.-W. Park, ‘‘Development of a ZVT- PWM buck cascaded buck–boost PFC converter of 2 kW with the widest range of input voltage,’’ IEEE Trans. Ind. Electron., vol. 65, no. 3, pp. 2090–2099, Mar. 2018.
6. C.-C. Lin, L.-S. Yang, and G. W. Wu, ‘‘Study of a non isolated bidirectional DC–DC converter,’’ IET Power Electron., vol. 6, no. 1, pp. 30–37, Jan. 2013.
7. M. A. Khan, A. Ahmed, I. Husain, Y. Sozer, and M. Badawy, ‘‘Performance analysis of bidirectional DC–DC converters for electric vehicles,’’ IEEE Trans. Ind. Appl., vol. 51, no. 4, pp. 3442–3452, Jul. 2015
8. S. Dusmez, A. Khaligh, and A. Hasanzadeh, ‘‘A zero voltage-transition bidirectional DC/DC converter,’’ IEEE Trans. Ind. Electron., vol. 62, no. 5, pp. 3152 3162, May 2015
9. H. Zhu, D. Zhang, B. Zhang, and Z. Zhou, ‘‘A nonisolated three-port DC–DC converter and three domain control method for PV-battery power systems,’’ IEEE Trans. Ind. Electron., vol. 62, no. 8, pp. 4937 4947, Aug. 2015.
10. M. B. Camara, H. Gualous, F. Gustin, and A. Berthon, ‘‘Design and new control of DC/DC converters to share energy between supercapacitors and batteries in hybrid vehicles,’’ IEEE Trans. Veh. Technol., vol. 57, no. 5, pp. 2721–2735,Sep.2008